

# $D$ - meson production at very forward rapidities: estimating the intrinsic charm contribution.

F. Carvalho<sup>†</sup>, A.V. Giannini<sup>‡</sup>, V.P. Gonçalves<sup>§</sup> and F.S. Navarra<sup>‡</sup>

<sup>†</sup> *Universidade Federal de São Paulo  
CEP 01302-907, São Paulo, Brazil*

<sup>‡</sup> *Instituto de Física, Universidade de São Paulo  
C.P. 66318, 05315-970 São Paulo, SP, Brazil and*

<sup>§</sup> *Instituto de Física e Matemática,  
Universidade Federal de Pelotas  
Caixa Postal 354, CEP 96010-900, Pelotas, RS, Brazil*

We study  $D$  - meson production at forward rapidities taking into account the non - linear effects in the QCD dynamics and the intrinsic charm component of the proton wave function. The total cross section, the rapidity distributions and the Feynman -  $x$  distributions are calculated for  $pp$  collisions at different center of mass energies. Our results show that, at the LHC, the intrinsic charm component changes the  $D$  rapidity distributions in a region which is beyond the coverage of the LHCb detectors. At higher energies the IC component dominates the  $y$  and  $x_F$  distributions exactly in the range where the produced  $D$  mesons decay and contribute the most to the prompt atmospheric neutrino flux measured by the ICECUBE Collaboration. We compute the  $x_F$  - distributions and demonstrate that they are enhanced at LHC energies by approximately one order of magnitude in the  $0.2 \leq x_F \leq 0.8$  range.

PACS numbers:

Keywords: Intrinsic charm, Particle production, Color Glass Condensate Formalism

## I. INTRODUCTION

The production of charm mesons in  $pp/pA/AA$  collisions is an important part of the physics program at the LHC and future colliders [1]. One of the reasons to study charm quark production is that it is expected to be sensitive to the non - linear effects of the QCD dynamics [2–6], which are predicted to be enhanced at forward rapidities. Another reason is that the understanding of open charm meson production is fundamental to estimate the magnitude of the prompt neutrino contribution to the atmospheric neutrino flux [7–11]. The latter is an important background for the astrophysical neutrino flux that can be measured by ICECUBE [13]. As demonstrated e.g. in Ref. [10, 11] and recently discussed in detail in Ref. [12], the main contribution to the prompt neutrino flux comes from open charm meson production at very forward rapidities, beyond that reached at the LHC, where new effects may be present.

One of the possible new effects that can contribute to open heavy meson production at forward rapidities is the presence of intrinsic heavy quarks in the hadron wave function (For recent reviews see, e.g. Refs. [14–17]). Heavy quarks in the sea of the proton can be perturbatively generated by gluon splitting. Quarks generated in this way are usually denoted *extrinsic* heavy quarks. In contrast, the *intrinsic* heavy quarks have multiple connections to the valence quarks of the proton and thus are sensitive to its nonperturbative structure. Most of the charm content of the proton sea is extrinsic and comes from the DGLAP [18] evolution of the initial gluon distribution. This process is well understood in perturbative QCD. The existence of the intrinsic charm (IC) component was first proposed long ago in Ref. [19] (see also Ref. [20]) and since then other models for IC have been discussed.

In the original model [19, 21], the creation of the  $c\bar{c}$  pair was studied in detail. It was assumed that the nucleon light cone wave function has higher Fock states, one of them being  $|qqq\bar{c}\bar{c}\rangle$ . The probability of finding the nucleon in this configuration is given by the inverse of the squared invariant mass of the system. Because of the heavy charm mass, the probability distribution as a function of the quark fractional momentum,  $P(x)$ , is very hard, as compared to the one obtained through the DGLAP evolution. In the literature this model is known as BHPS. A more dynamical approach is given by the meson cloud model (MC). In this model, the nucleon fluctuates into an intermediate state composed by a charmed baryon plus a charmed meson [22, 23]. The charm is always confined in one hadron and carries the largest part of its momentum. In the hadronic description we can use effective lagrangians to compute the charm splitting functions, which turn out to favor harder charm quarks than the DGLAP ones. The main difference between the BHPS and MC models is that the latter predicts that the charm and anticharm distributions are different

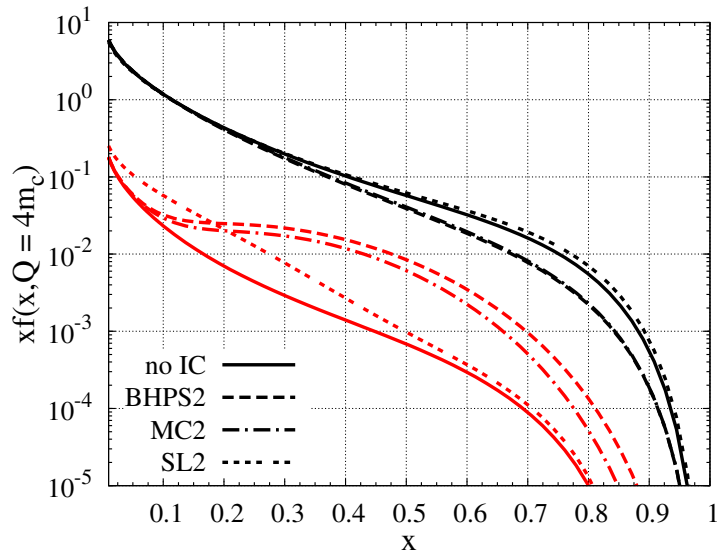


FIG. 1: Predictions of the different intrinsic charm models for the  $x$  - dependence of the charm (lower red curves) and gluon (upper black curves) distributions as obtained by the CTEQ Collaboration [25].

[24], since they carry information about the hadronic bound states in which the quarks are.

The intrinsic charm (IC) component of the proton wave function was considered in the global analysis performed in 2006 by the CTEQ collaboration [25]. In this update the CTEQ group determined the normalization of the IC distribution. In fact, they find several IC distributions which were compatible with the world data. Apart from the already mentioned BHPS and meson cloud models, the CTEQ group has tested another model of intrinsic charm, called sea-like IC. It consists basically in assuming that at a very low resolution (before the DGLAP evolution) there is already some charm in the nucleon, which has a typical sea quark momentum distribution ( $\simeq 1/\sqrt{x}$ ) with normalization to be fixed by fitting data. The resulting charm distributions are presented in Fig. 1 (lower red curves), where the no IC curve represents the standard CTEQ prediction, obtained disregarding the presence of intrinsic charm in the initial condition of the evolution. The BHPS and MC models predict a large enhancement of the distribution at large  $x$  ( $> 0.1$ ). In contrast, the sea-like (SL) model predicts a smaller enhancement at large  $x$ , but a larger one at smaller  $x$  ( $< 0.2$ ). We follow Ref. [25] and use the labels BHPS2, MC2 and SL2 for the versions of these models which have the maximum amount of intrinsic charm. In Fig. 1 we also present the corresponding gluon distributions (upper black curves). Due to the momentum sum rule, the gluon distribution is also modified by the inclusion of intrinsic charm. In particular, the BHPS and MC models imply a suppression in the gluon distribution at large  $x$  (For a more detailed discussion see e.g. Ref. [26]).

The large enhancement at large -  $x$  in the charm distribution, associated to intrinsic charm, has motivated a large number of phenomenological studies to confirm the presence (or absence) of this component in the hadron wave function. One of the most direct consequences is that the intrinsic charm component gives rise to heavy mesons with large fractional momenta relative to the beam particles, affecting the Feynman -  $x$  ( $x_F$ ) and rapidity distribution of charmed particles. This aspect was explored e.g. in Refs. [27–29]). Moreover, the presence of intrinsic charm changes the Higgs [30] and photon production [31] at high  $x_F$ . Over the last two years, new parametrizations of the IC distribution were released [32, 33], motivating an intense debate about the amount of IC in the proton wave function [33, 35]. At the same time new implications of IC were discussed [36–38]. In particular, in Ref. [38] the authors presented a method to generate matched intrinsic charm / intrinsic bottom distributions for any PDF set without the need for a complete global re-analysis. This allows one to easily carry out a consistent analysis including intrinsic quark effects. Additionally, the proposal of constructing a high energy and high luminosity fixed-target experiment using the LHC beams (AFTER@LHC) [39] motivated new theoretical studies about the possibility of measuring the intrinsic charm component of the nucleon [16]. Finally, the effect of IC on the atmospheric neutrino flux measured by ICECUBE was addressed in Refs. [11, 40, 41] considering different phenomenological models for the treatment of the intrinsic component.

In this paper we revisit  $D$  - meson production at forward rapidities in hadronic collisions, which probes particle production at large  $x_F$ . In this case, the kinematics is very asymmetric, with the hadrons in the final state emerging from collisions of projectile partons with large light cone momentum fractions with target partons carrying a very

small momentum fraction. As a consequence, we have the scattering of a dilute projectile on a dense target, where the small- $x$  effects coming from the non-linear aspects of QCD and from the physics of the Color Glass Condensate (CGC) [42] are expected to appear and the usual factorization formalism is expected to breakdown [3]. The satisfactory description of the experimental data in this kinematical region with the CGC approach [43–45] indicates that the CGC is the appropriate framework to study particle production in the large rapidity region (for an alternative approach, see [46]). Along this line, in [28] the formalism proposed in [43] for light meson production was generalized to  $D$ -meson production in  $pp$  and  $pA$  collisions at forward rapidities, including intrinsic charm quarks in the projectile wave function. Recently, the basic equation proposed in Ref. [28] was reobtained in Ref. [6]. In Ref. [28] we have presented predictions for the  $p_T$  distributions of  $D$  mesons at large rapidities considering  $pp$  and  $pA$  collisions at RHIC and LHC energies. Our results indicated that the presence of intrinsic charm strongly modifies the  $p_T$  - spectra. However, a shortcoming of Ref. [28] is that the gluonic contribution to  $D$  - meson production, associated to the  $g + g \rightarrow c + \bar{c}$  channel, was not included in a systematic way. Basically, this contribution was considered as a background and was estimated considering the standard PYTHIA predictions. One of the main goals of this paper is to consistently include this contribution, taking into account the non - linear effects in the QCD dynamics at small  $x$ , as well as the modifications at large  $x$  in the gluon distribution predicted by the different IC models. We will present predictions for the total cross section and rapidity distribution considering  $pp$  - collisions at LHC energies and compare them with the recent experimental data. In particular, we will estimate the rapidity region where the IC contribution is larger. Another goal is to estimate the impact of the IC component on the  $x_F$  - distributions, which are the main input in the calculations of the prompt neutrino flux. We will present our predictions for this distribution considering LHC and Ultra - High Cosmic Rays (UHECR) energies and demonstrate that the  $x_F$  behavior is strongly modified in the  $x_F \geq 0.2$  range.

This paper is organized as follows. In next Section we will present a brief review of the main ingredients used in our calculation of  $D$  - meson production at forward rapidities and large  $x_F$ . In particular, we review the approach proposed in Ref. [28] for the intrinsic component and the dipole picture of heavy quark production in gluonic interactions developed in Refs. [47, 48] and applied at the LHC in Refs. [4, 49]. Both contributions will be expressed in terms of the dipole - nucleon scattering amplitude, which we will assume to be given by the model proposed in Ref. [44] and recently updated to describe the recent LHC data on forward particle production in  $pp$  collisions in Ref. [45]. In Section III we present our results for the total cross section and rapidity distribution and compare with recent experimental data. The impact of the IC contribution is estimated and the optimal kinematical range to probe its presence is determined. Moreover, we estimate the  $x_F$  - distribution considering  $pp$  collisions at LHC and UHECR energies. Finally, in Section IV we summarize our main conclusions.

## II. $D$ - MESON PRODUCTION AT FORWARD RAPIDITIES

In what follows we will address prompt  $D$  - meson production, disregarding the contribution from the decay of heavier mesons. In this case, the  $D$  - meson production is determined by the cross section of heavy quark production, which is usually described in the collinear or  $k_T$ -factorization frameworks of QCD. Using collinear factorization, charm production is described in terms of the basic subprocesses of gluon fusion ( $g + g \rightarrow c + \bar{c}$ ) and light quark-antiquark fusion ( $q + \bar{q} \rightarrow c + \bar{c}$ ), with the latter being negligible at high energies. The elementary cross section computed to leading order (LO) or next-to-leading order (NLO) is folded with the corresponding parton distributions and fragmentation functions. This is the basic procedure in most of the calculations performed, for instance, with the standard codes PYTHIA and MCFM. However, at small  $x$  collinear factorization should be generalized to resum powers of  $\alpha_s \ln(s/q_T^2)$ , where  $q_T$  is the transverse momentum of the final state and  $\sqrt{s}$  is the center of mass energy. This resummation is done in the  $k_T$ -factorization framework, where the cross section is expressed in terms of unintegrated gluon distributions which are determined by the QCD dynamics at small- $x$  (For recent results see e.g. Ref. [50]). The presence of non - linear effects in the QCD dynamics is expected to have impact on heavy quark production at high energies [2–5], leading to the breakdown of the  $k_T$ -factorization [3, 51].

One way to study heavy quark production in gluon - gluon interactions is the color dipole formalism developed in Refs. [47, 48], which allows us to take into account the non - linear effects in the QCD dynamics as well as higher order corrections [52]. The basic idea of this approach is that, before interacting with the hadron target, a gluon is emitted by the projectile and fluctuates into a color octet pair  $Q\bar{Q}$ . The dipole picture of HQ production is represented in Fig. 2 (left panel). Taking into account that the heavy quarks in the dipole as well the incident gluon (before fluctuating into the pair) can interact with the target, the rapidity distribution for a  $h_1 h_2$  collision can be expressed as follows [48]:

$$\frac{d\sigma(h_1 h_2 \rightarrow \{Q\bar{Q}\}X)}{dy} = x_1 G^{h_1}(x_1, \mu_F^2) \sigma(G h_2 \rightarrow \{Q\bar{Q}\}X), \quad (1)$$

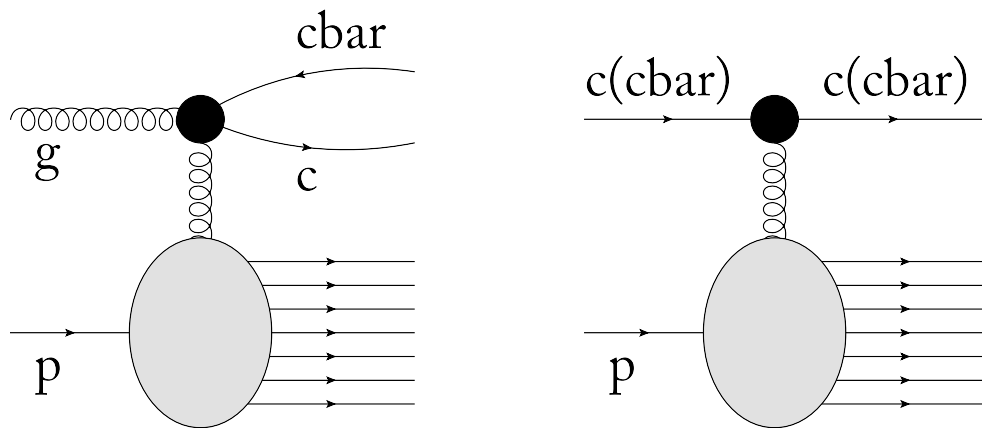


FIG. 2: Contributions to  $D$  - meson production at forward rapidities. Left panel: Contribution from gluon - gluon interactions. Right panel: Contribution from charm in the initial state.

where  $x_1 G_p(x_1, \mu_F)$  is the projectile gluon distribution, the cross section  $\sigma(Gh_2 \rightarrow \{Q\bar{Q}\}X)$  describes heavy quark production in a gluon - nucleon interaction,  $y$  is the rapidity of the pair and  $\mu_F$  is the factorization scale. Moreover, the cross section of the process  $G + h_2 \rightarrow Q\bar{Q}X$  is given by:

$$\sigma(Gh_2 \rightarrow \{Q\bar{Q}\}X) = \int_0^1 d\alpha \int d^2\rho |\Psi_{G \rightarrow Q\bar{Q}}(\alpha, \rho)|^2 \sigma_{q\bar{q}G}^{h_2}(\alpha, \rho) \quad (2)$$

where  $\alpha$  ( $\bar{\alpha} \equiv 1 - \alpha$ ) is the longitudinal momentum fraction carried by the quark (antiquark),  $\vec{\rho}$  is the transverse separation of the pair,  $\Psi_{G \rightarrow Q\bar{Q}}$  is the light-cone (LC) wave function of the transition  $G \rightarrow Q\bar{Q}$  (which is calculable perturbatively and is proportional to  $\alpha_s$ ) and  $\sigma_{Q\bar{Q}G}^{h_2}$  is the scattering cross section of a color neutral quark-antiquark-gluon system on the hadron target  $h_2$  [47, 48, 52]. The three - body cross section is given in terms of the dipole - nucleon cross section  $\sigma_{q\bar{q}}$  as follows:

$$\sigma_{q\bar{q}G}^{h_2}(\alpha, \rho) = \frac{9}{8} [\sigma_{q\bar{q}}(\alpha\rho) + \sigma_{q\bar{q}}(\bar{\alpha}\rho)] - \frac{1}{8} \sigma_{q\bar{q}}(\rho) . \quad (3)$$

The dipole - nucleon cross section can be expressed in terms of the forward scattering amplitude  $\mathcal{N}(x, \rho)$ , which is determined by the QCD dynamics and constrained by the HERA data, as follows:

$$\sigma_{q\bar{q}}(x, \rho) = \sigma_0 \mathcal{N}(x, \rho) \quad (4)$$

where  $\sigma_0$  is a free parameter usually determined by a fit of the HERA data. In the dipole picture the heavy quark production cross section is associated to gluon - gluon interactions and it is determined by the projectile gluon distribution and by the model assumed for the dipole - nucleon scattering amplitude. Moreover, it depends on the values of the charm mass and of the running coupling constant  $\alpha_s$ . Finally, in order to estimate the corresponding  $D$  - meson cross section we need to convolute the heavy quark cross section with the fragmentation function, for which a model must be chosen.

As discussed in the Introduction, the cross sections at forward rapidities are dominated by collisions of projectile partons with large light cone momentum fractions with target partons carrying a very small momentum fraction. From light hadron production, we know [53] that in this kinematical range the cross section is dominated by the interaction of valence quarks of the projectile with gluons of the target. In other words, the cross section depends on the partonic structure of the projectile at large- $x$ . If the intrinsic charm is present in the proton wave function and strongly modifies the behavior of the corresponding parton distribution at large  $x$ , it is natural to expect that IC may change the  $D$ -meson production cross section. Additionally, as we are probing very small values of  $x$  in the target, non - linear effects in QCD dynamics should be taken into account. These were the basic motivations of the study performed in Ref. [28], where we generalized the DGLAP  $\otimes$  CGC factorization scheme proposed in Ref. [43] to estimate the intrinsic charm contribution (For a recent derivation see Ref. [6]). In this approach the projectile (dilute system) evolves according to the linear DGLAP dynamics and the target (dense system) is treated using the CGC formalism. As a consequence the differential cross section of  $D$  - meson production associated to charm in the initial

state is given by [28]

$$\frac{d\sigma}{dyd^2p_T} = \frac{1}{(2\pi)^2} \int_{x_F}^1 \frac{dz}{z^2} f_{c/p}(x_1, q_T^2) \sigma_0 \tilde{\mathcal{N}}\left(x_2, \frac{p_T}{z}\right) D_{D/c}(z, \mu_{FF}^2). \quad (5)$$

with the variables  $x_F$  e  $x_{1,2}$  being defined by  $x_F = \sqrt{p_T^2 + m^2} e^y / \sqrt{s}$  and  $x_{1,2} = q_T e^{\pm y} / \sqrt{s}$ , where  $q_T = p_T/z$ . Therefore, particle production at forward rapidities and small values of transverse momentum is characterized by the interaction between partons with large  $x_1$  in the projectile and small values of  $x_2$  in the target. As a consequence, the hadron in the final state is expected to be produced at large values of  $x_F$ . Moreover,  $f_{c/p}$  represents the projectile charm distribution,  $D_{D/c}$  is the charm fragmentation function in a  $D$  - meson and  $\tilde{\mathcal{N}}(x, k_T)$  is the Fourier transform of the scattering amplitude  $\mathcal{N}(x, \rho)$ . The basic diagram associated to this process is presented in Fig. 2 (right panel). In Ref. [28] we estimated the  $p_T$  - spectra of the  $D$  - mesons produced at different rapidities in  $pp$  and  $pA$  collisions at RHIC and LHC energies and demonstrated that the IC component in the proton wave function implies a strong enhancement of the differential cross sections in comparison with the predictions derived disregarding this component. In the next Section we will extend the analysis performed in Ref. [28], calculating the corresponding rapidity and  $x_F$  - distributions and including the contribution of gluon-gluon interactions to  $D$ -meson production. In order to be theoretically consistent, we will estimate Eqs. (1) and (5) using a common pdf set for the gluon and charm distributions as well the same models for the scattering amplitude and fragmentation function.

### III. RESULTS AND DISCUSSION

In what follows we will present our predictions for  $D$ -meson production at forward rapidities and large -  $x_F$  considering the two contributions discussed in the previous Section. This kinematical region is characterized by large values of  $x_1$  and small  $x_2$ , which implies an asymmetric projectile – target configuration, usually denoted dilute – dense one. It is exactly for this configuration that the dipole approaches for heavy quark production considered in our analysis have been derived [28, 43, 48]. In order to calculate the cross sections we need to specify the parametrization used for the parton distributions, the model for the scattering amplitude and the  $c \rightarrow D$  fragmentation function. Moreover, the results depend on the charm mass, on the factorization scale and on the running coupling constant.

Let us start discussing the model assumed for the scattering amplitude  $\mathcal{N}(x, \rho)$  and, consequently, for  $\tilde{\mathcal{N}}(x, k_T)$ . This quantity involves the QCD dynamics at high energies and contains all the information about the initial state of the hadronic wavefunction and therefore about the non-linearities and quantum effects which are characteristic of a system such as the CGC (For reviews, see e.g. [42]). Formally its evolution is usually described in the mean field approximation of the CGC formalism by the BK equation [54]. Its analytical solution is known only in some special cases. Advances have been made in solving the BK equation numerically [55]. Since the BK equation still lacks a formal solution in all phase space, several groups have constructed phenomenological models for the dipole scattering amplitude. These models have been used to fit the RHIC and HERA data [43, 44, 56]. In general, it is assumed that  $\mathcal{N}$  can be modelled through a simple Glauber-like formula,

$$\mathcal{N}(x, \rho) = 1 - \exp\left[-\frac{1}{4}(\rho^2 Q_s^2(x))^{\gamma(x, \rho^2)}\right], \quad (6)$$

where  $Q_s(x)$  is the saturation scale,  $\gamma$  is the anomalous dimension of the target gluon distribution and  $\rho$  is the dipole size. The speed with which we move from the non-linear regime to the extended geometric scaling regime and then from the latter to the linear regime is what differs one phenomenological model from another. This transition speed is dictated by the behavior of the anomalous dimension  $\gamma(x, \rho^2)$ . In this paper we consider the BUW [44] dipole model, which assumes that the anomalous dimension can be expressed by

$$\gamma_{BUW} = \gamma_s + (1 - \gamma_s) \frac{(\omega^a - 1)}{(\omega^a - 1) + b} \quad (7)$$

where  $\omega = q_T/Q_s$  and  $a, b$  and  $\gamma_s$  are free parameters to be fixed by fitting experimental data. In the BUW Ansatz, the anomalous dimension  $\gamma$  leads to geometric scaling and hence depends only on the ratio  $\omega = q_T/Q_s$  but not separately on  $q_T$  and on  $Q_s(x)$ . Recently, in Ref. [45], the original parameters of the BUW model were updated in order to make this model compatible with all existing data. In particular, the recent LHC data on light hadron production at forward rapidity are satisfactorily reproduced by the updated model. In what follows we will use the BUW model with the parameters obtained in Ref. [45].

In order to quantify the impact of the intrinsic charm considering the largest possible number of models of this component, we will use in our calculations the leading order CTEQ 6.5 parametrization for the parton distributions

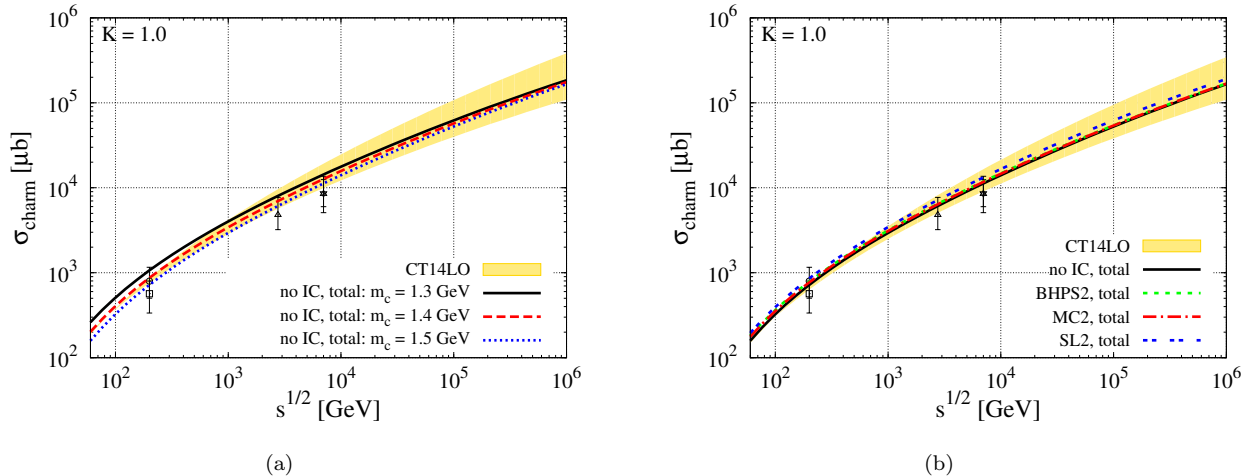


FIG. 3: Energy dependence of the total charm production cross section considering (a) different values of the charm mass, and (b) different models of the intrinsic charm component. Data from Refs. [57, 58, 61–64].

[25]. This particular parametrization has two different PDF sets for each of the models discussed in the Introduction (BHPS, MC and SL), considering different amounts of intrinsic component. It is important to emphasize that this amount is still subject of intense debate. The recent IC global analysis presented in [33] comes to the conclusion that such a big amount of IC in the proton is excluded by the current experimental data. Depending on the analysis, the obtained upper limit on the IC normalization is around 2.5 % or 0.5 %. As our goal is highlighting the possible effect of IC, we will only present the predictions obtained with the CTEQ 6.5 parametrization with the maximum amount of IC ( $\simeq 3.5$  %) for a given model (denoted BHPS2, MC2 and SL2 hereafter).

It is important to emphasize that the CTEQ-TEA group has also performed a global analysis of the recent experimental data including an intrinsic charm component, which is available in the CT14 parametrization [32]. However, this analysis has been performed at next-to-next-to-leading order and the meson cloud model was not considered. As the basic equations used in our study of  $D$  - meson production have been derived at leading order, we believe that it is more consistent to use in our calculations PDFs obtained at the same order. In order to analyse the influence of a more recent leading order parametrization, we will also present in some of our results, the predictions obtained using the CT14 LO parametrization, which disregards the intrinsic component. Following Ref. [10] we will use the fragmentation function from Ref. [59] given by:

$$D_c^h(z) = \frac{Nz(1-z)^2}{[(1-z)^2 + \epsilon z]^2}. \quad (8)$$

where  $N = 0.577$  and  $\epsilon = 0.101$  and the fragmentation fraction into  $D^0$  is 0.606. An alternative is to consider fragmentation functions with DGLAP evolution as e.g. those obtained in Ref. [60]. However, as demonstrated in Ref. [49], the main implication of DGLAP evolution is the modification of the  $p_T$  - spectra at large transverse momenta. In our analysis we are interested in the rapidity distribution, which is dominated by small values of  $p_T$ . Therefore, the DGLAP evolution effects in the fragmentation function are expected to have a negligible impact on  $d\sigma/dy$ . We also will assume that the factorization scale  $\mu_F$  in Eq. (1) is equal to  $\mu_F^2 = 4 \cdot m_c^2$  and that  $\alpha_s = \alpha_s(\mu_F^2)$ . As a consequence, our predictions depend only on the choice of the charm mass. Finally, it is important to emphasize that our predictions for the gluon and charm contributions, given by the Eqs. (1) and (5), could be modified by higher order corrections, which are in several cases mimicked by a  $K$  - factor multiplying the expressions, fitted to describe the data. In our analysis, we will assume that  $K = 1$ . However, the estimate of higher corrections for the gluonic and charm contributions is a subject that deserves a more detailed study in the future.

In Fig. 3 (a) we show our results for the total charm production cross section, considering different values of the charm mass, summing the gluonic and charm contributions and assuming that the gluon and charm PDFs are given by the standard CTEQ 6.5 parametrization without an intrinsic component. We compare our predictions with the experimental data. We can observe that the data at high energies are reasonably well described. In what follows we will assume that  $m_c = 1.5$  GeV. For comparison we also present the CT14 LO predictions for  $m_c = 1.5$  GeV and different values for the factorization scale  $\mu_F$ , in order to estimate the dependence of our predictions on the choice of this scale. Considering the range  $m_c^2 \leq \mu_F^2 \leq 16 m_c^2$ , we observe that the CT14 LO parametrization leads to the band presented in Fig. 3, which demonstrates that the high energy behavior of the cross section is strongly dependent on the choice of  $\mu_F$ . In Fig. 3 (b) we investigate the impact of the different IC models on the total charm cross

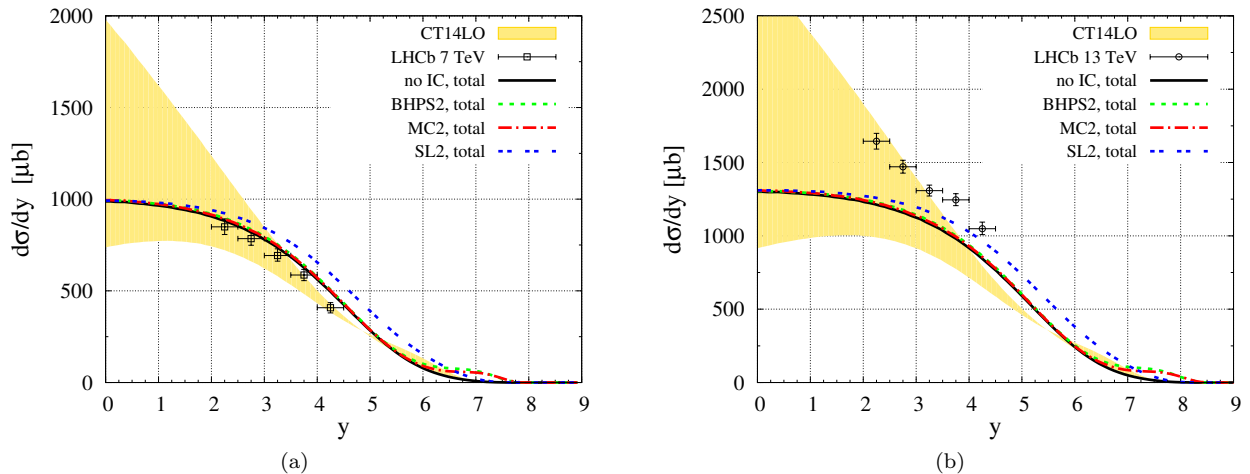


FIG. 4: Rapidity distribution of  $D^0 + \bar{D}^0$  mesons produced in  $pp$  collisions at (a)  $\sqrt{s} = 7$  TeV and (b)  $\sqrt{s} = 13$  TeV. Data from Refs. [57, 58].

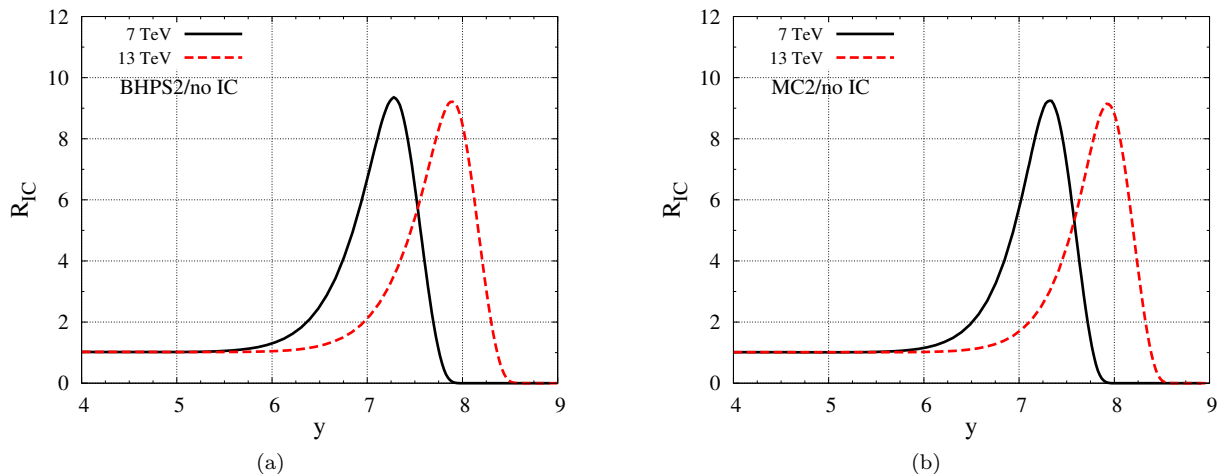


FIG. 5: Rapidity dependence of the ratio between the IC predictions and the standard CTEQ 6.5 parametrization without intrinsic charm: a) BHPS2. b) MC2.

section. We can see that the different predictions are almost identical, which is expected, since the total cross section is dominated by the contribution associated to charm production at central rapidities, where both  $x$  values of the partons involved in the collision are small. As a consequence, the modifications associated to the presence of intrinsic charm are negligible for this observable.

Our predictions for the rapidity distribution of  $D^0 + \bar{D}^0$  mesons, produced in  $pp$  collisions at  $\sqrt{s} = 7$  and 13 TeV, are presented in Figs. 4 (a) and (b), respectively. Considering the CT14 LO predictions, we can see that the predictions at central rapidities are strongly sensitive to the choice of  $\mu_F$ , with the uncertainty decreasing at larger rapidities, which is the kinematical range where the IC component contributes. The standard CTEQ 6.5 and the BHPS2 and MC2 models predict a similar behavior at small rapidities, differing only at very forward rapidities. On the other hand, the SL2 model predicts an enhancement in the rapidity distribution in the region of intermediate values of  $y$ , which is directly associated to the enhancement of the charm distribution for  $x \leq 0.2$  (See Fig. 1). In order to quantify the influence of the intrinsic component and determine the kinematical region affected by its presence, in Fig. 5 we present the rapidity dependence of the ratio between the IC predictions and the standard CTEQ 6.5 one without an intrinsic component (denoted no IC). Our results demonstrate that the intrinsic component modifies the rapidity distribution at very forward rapidities, beyond those reached by the LHCb Collaboration. We observe that the distribution can be enhanced by a factor  $\approx 8$ , with the position of the maximum shifting to larger rapidities with the growth of the center of mass energy. This behavior can be easily understood if we remember that the  $x$  - values probed in the projectile are approximately  $x \approx (m_T/\sqrt{s}) \exp(+y)$ , where  $m_T = \sqrt{4m_c^2 + p_T^2}$ . Consequently, when the energy increases, we need to go to larger rapidities in order to reach the same value of  $x$ .

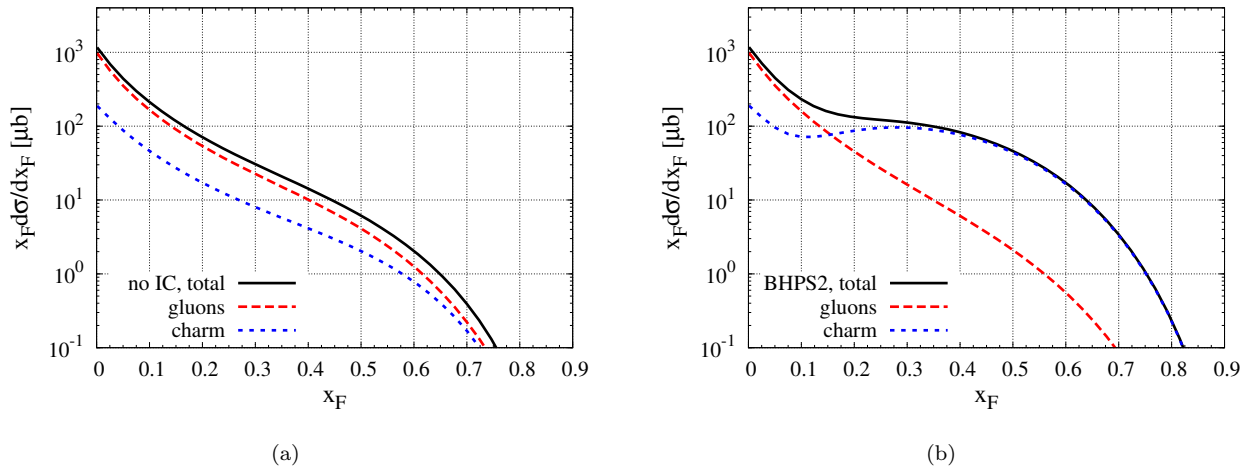


FIG. 6: Feynman -  $x$  distributions of the produced  $D^0 + \bar{D}^0$  mesons in  $pp$  collisions at  $\sqrt{s} = 13$  TeV considering: (a) the standard CTEQ 6.5 parametrization and (b) the BHPS model. The gluonic and charm contributions are presented separately.

Although the intrinsic component is predicted to manifest itself in a rapidity region beyond the current kinematical rapidity range probed by the LHC, it may also have implications for other observables. As already emphasized in Ref. [28], the IC component modifies the  $p_T$  spectra for a fixed rapidity. In particular, we can access large values of  $x$  in the projectile wave function by increasing the transverse momentum for a fixed  $y$ . However, the clear identification of the intrinsic component is a hard task, since the  $p_T$  spectra can also be modified e.g. by higher order corrections. Another observable that can be affected by the IC component is the prompt atmospheric neutrino flux, which is strongly dependent on the features of  $D$  - meson production at very forward rapidities (For a recent detailed discussion see Ref. [10–12]). As demonstrated in Ref. [12], the main contribution to the neutrino flux comes from rapidities beyond the LHCb range, exactly where we predict the largest impact of IC. As one of the main ingredients to calculate the prompt neutrino flux associated to the decay of open charm mesons is the Feynman  $x$  - distribution, in what follows we will analyse in more detail the influence of the IC on this distribution for different energies. In Fig. 6 we show our predictions for the  $x_F$  - distribution of  $D^0 + \bar{D}^0$  mesons, produced in  $pp$  collisions at  $\sqrt{s} = 13$  TeV. We present separately the gluon and charm contributions, as well as the sum of the two terms, denoted “total” in the figures. For comparison we present in Fig. 6 (a) the standard CTEQ 6.5 predictions, which are obtained disregarding a possible intrinsic charm in the initial conditions of the DGLAP evolution. In this case, the charm contribution is smaller than the gluonic one for all values of  $x_F$ , and the distribution is dominated by the production of  $D$  mesons in gluon - gluon interactions. In contrast, when intrinsic charm is included, the behavior of the distribution in the intermediate  $x_F$  range ( $0.2 \leq x_F \leq 0.8$ ) is strongly modified, as we can see in Fig. 6 (b), where we present the BHPS2 predictions. In order to analyse the energy dependence of the  $x_F$  - distribution, in Fig. 7 we present our predictions for this distribution considering  $pp$  collisions at (a)  $\sqrt{s} = 13$  TeV and (b)  $\sqrt{s} = 200$  TeV. The latter value is equivalent to the energy probed when ultra - high energy cosmic rays interact with the atmosphere. We have checked that the BHPS2 and MC2 predictions are similar for all energies considered. In order to determine the magnitude of the impact of the IC and the kinematical range influenced by its presence, we present in Fig. 8 (a) and (b) our predictions for the ratio between the  $x_F$  distributions predicted by the BHPS and MC models and the standard CTEQ 6.5 one. As expected from Fig. 7, the BHPS and MC models predict an enhancement at intermediate  $x_F$  and a suppression at very large  $x_F$ . Moreover, the magnitude of the enhancement is similar for both models, being a factor 6 – 9 in the energy ranges considered. The main aspect that should be emphasized here is that *the enhancement occurs exactly in the  $x_F$  range where the contribution of  $D$  - mesons to the prompt neutrino flux [10–12] is dominant*. Consequently, we expect that the presence of the IC component will modify the predictions for the prompt atmospheric neutrino flux. This expectation will be analysed in detail in a future publication.

#### IV. CONCLUSIONS

A complete knowledge of the partonic structure of hadrons is fundamental to make predictions for the Standard Model and beyond Standard Model processes at hadron colliders. In particular, the heavy quark contribution to the proton structure has a direct impact on several observables analysed at the LHC. Direct measurements of heavy flavors in DIS and hadronic colliders are consistent with a perturbative origin. However, these experiments are in general not



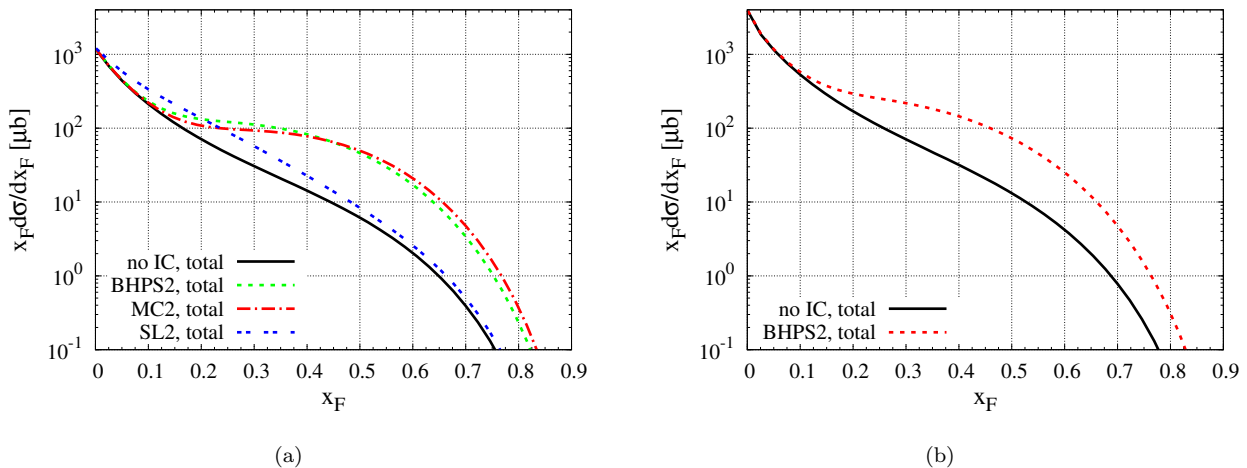


FIG. 7: Feynman -  $x$  distributions of the produced  $D^0 + \bar{D}^0$  mesons in  $pp$  collisions at (a)  $\sqrt{s} = 13$  TeV and (b)  $\sqrt{s} = 200$  TeV considering different models for the intrinsic component.

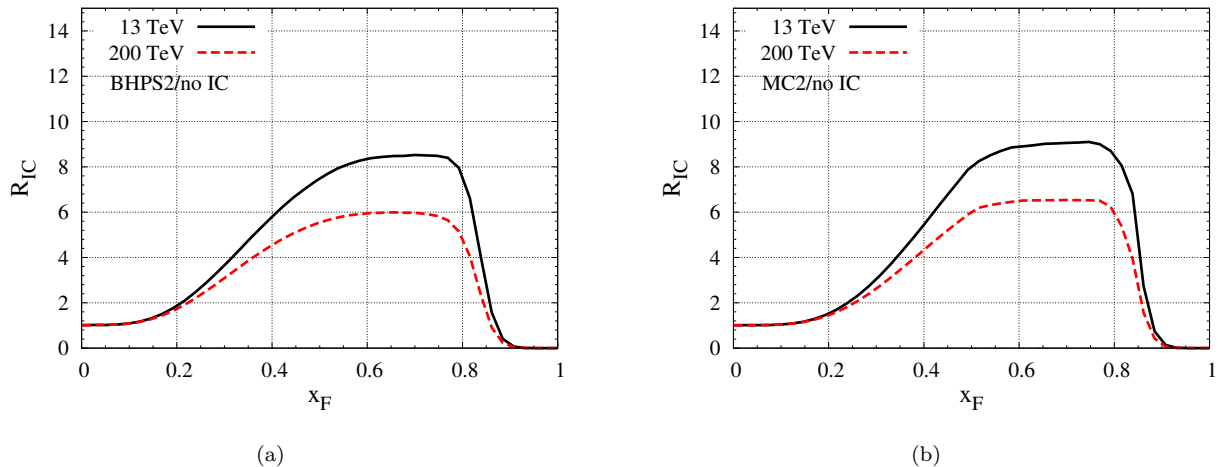


FIG. 8: Feynman -  $x$  dependence of the ratio between the IC predictions and the standard CTEQ 6.5 parametrization. a) BHPS2. b)MC2.

sensitive to heavy quarks at large  $x$ . Therefore, it is fundamental to propose and study other observables which may be used to determine the presence (or absence) of an intrinsic heavy quark component in the hadron wave function. In recent years, a series of studies have discussed in detail how to probe this intrinsic component, with particular emphasis in processes that are strongly sensitive to the charm in the initial state. One of this processes is  $D$  - meson production at forward rapidities, which is also influenced by the specific features of QCD dynamics at high energies. In this paper we have extended the approach proposed in Ref. [28] to the production of  $D$  - mesons from charm quarks present in the initial state and we have calculated the rapidity and  $x_F$  - distributions of  $D$  - meson produced in  $pp$  collisions at the LHC and in interactions at higher energies. In particular, we have included the contribution associated to gluon - gluon interactions, which are also affected by the intrinsic charm component. Considering different models of the intrinsic charm component, we have demonstrated that the rapidity range influenced by IC is beyond that reached by the LHCb Collaboration. However IC is important for the calculation of the prompt neutrino flux. Our results indicated that the  $x_F$  - distribution is enhanced by the intrinsic component in the kinematical range that dominates the  $D$  - meson contribution to the prompt neutrino flux. Consequently, the inclusion of the IC contribution in the corresponding calculations can be important to estimate the prompt atmospheric neutrino flux probed by the ICECUBE.

## Acknowledgments

VPG thanks Anna Stasto, Roman Pasechnik, Antoni Szczurek and Rafal Maciula for useful discussions about the  $D$ -meson production at high energies and its implications on the prompt neutrino flux. FSN is grateful to Juan Rojo and J.P. Lansberg for useful discussions. This work was partially financed by the Brazilian funding agencies CAPES, CNPq, FAPESP and FAPERGS.

- 
- [1] A. Andronic *et al.*, Eur. Phys. J. C **76**, 107 (2016).
  - [2] D. Kharzeev and K. Tuchin, Nucl. Phys. A **735**, 248 (2004).
  - [3] K. Tuchin, Phys. Lett. B **593**, 66 (2004); Nucl. Phys. A **798**, 61 (2008); Y. V. Kovchegov and K. Tuchin, Phys. Rev. D **74**, 054014 (2006); H. Fujii, F. Gelis and R. Venugopalan, J. Phys. G **34**, S937 (2007).
  - [4] E. R. Cazaroto, V. P. Goncalves and F. S. Navarra, Nucl. Phys. A **872**, 196 (2011).
  - [5] H. Fujii and K. Watanabe, Nucl. Phys. A **920**, 78 (2013).
  - [6] T. Altinoluk, N. Armesto, G. Beuf, A. Kovner and M. Lublinsky, Phys. Rev. D **93**, 054049 (2016).
  - [7] V. P. Goncalves and M. V. T. Machado, JHEP **0704**, 028 (2007).
  - [8] R. Enberg, M. H. Reno and I. Sarcevic, Phys. Rev. D **78**, 043005 (2008).
  - [9] M. V. Garzelli, S. Moch and G. Sigl, JHEP **1510**, 115 (2015).
  - [10] A. Bhattacharya, R. Enberg, Y. S. Jeong, C. S. Kim, M. H. Reno, I. Sarcevic and A. Stasto, JHEP **1611**, 167 (2016).
  - [11] R. Laha and S. J. Brodsky, arXiv:1607.08240.
  - [12] V. P. Goncalves, R. Maciula, R. Pasechnik and A. Szczurek, arXiv:1708.03775 [hep-ph].
  - [13] T. Gaisser and F. Halzen, Ann. Rev. Nucl. Part. Sci. **64**, 101 (2014).
  - [14] R. D. Ball *et al.* [NNPDF Collaboration], Eur. Phys. J. C **76**, 647 (2016).
  - [15] T. J. Hobbs, arXiv:1612.05686 [hep-ph].
  - [16] S. J. Brodsky, A. Kusina, F. Lyonnet, I. Schienbein, H. Spiesberger and R. Vogt, Adv. High Energy Phys. **2015**, 231547 (2015).
  - [17] S. J. Brodsky, V. A. Bednyakov, G. I. Lykasov, J. Smiesko and S. Tokar, arXiv:1612.01351 [hep-ph].
  - [18] Yu. Dokshitzer, Sov. Phys. JETP **46**, 641 (1977); V.N. Gribov and L.N. Lipatov, Sov. J. Nucl. Phys. **15**, 438 (1972); G. Altarelli and G. Parisi, Nucl. Phys. B **126**, 298 (1977).
  - [19] S. J. Brodsky, P. Hoyer, C. Peterson and N. Sakai, Phys. Lett. B **93**, 451 (1980).
  - [20] V. D. Barger, F. Halzen and W. Y. Keung, Phys. Rev. D **25**, 112 (1982).
  - [21] R. Vogt and S. J. Brodsky, Nucl. Phys. B **438**, 261 (1995); **478**, 311 (1996).
  - [22] S. Paiva, M. Nielsen, F. S. Navarra, F. O. Duraes and L. L. Barz, Mod. Phys. Lett. A **13**, 2715 (1998); F. S. Navarra, M. Nielsen, C. A. A. Nunes and M. Teixeira, Phys. Rev. D **54**, 842 (1996).
  - [23] F. M. Steffens, W. Melnitchouk and A. W. Thomas, Eur. Phys. J. C **11**, 673 (1999).
  - [24] F. Carvalho, F. O. Duraes, F. S. Navarra and M. Nielsen, Phys. Rev. Lett. **86**, 5434 (2001).
  - [25] J. Pumplin, H. L. Lai and W. K. Tung, Phys. Rev. D **75**, 054029 (2007).
  - [26] A. Alekhaneshvar, M. Goharipour and S. Rostami, Eur. Phys. J. A **52**, 352 (2016).
  - [27] G. Ingelman and M. Thunman, Z. Phys. C **73**, 505 (1997).
  - [28] V. P. Goncalves, F. S. Navarra and T. Ullrich, Nucl. Phys. A **842**, 59 (2010).
  - [29] B. A. Kniehl, G. Kramer, I. Schienbein and H. Spiesberger, Phys. Rev. D **79**, 094009 (2009).
  - [30] S. J. Brodsky, B. Kopeliovich, I. Schmidt and J. Soffer, Phys. Rev. D **73**, 113005 (2006).
  - [31] V. A. Bednyakov, M. A. Demichev, G. I. Lykasov, T. Stavreva and M. Stockton, Phys. Lett. B **728**, 602 (2014); P. H. Beauchemin, V. A. Bednyakov, G. I. Lykasov and Y. Y. Stepanenko, Phys. Rev. D **92**, 034014 (2015).
  - [32] S. Dulat, T.-J. Hou, J. Gao, J. Huston, J. Pumplin, C. Schmidt et al., Phys. Rev. D **89** 073004, (2014);
  - [33] P. Jimenez-Delgado, T. J. Hobbs, J. T. Londergan and W. Melnitchouk, Phys. Rev. Lett. **114**, 082002 (2015); Phys. Rev. Lett. **116**, 019102 (2016).
  - [34] T. J. Hobbs, J. T. Londergan and W. Melnitchouk, Phys. Rev. D **89**, 074008 (2014); R. D. Ball, V. Bertone, M. Bonvini, S. Carrazza, S. Forte et al., arXiv:1605.06515.
  - [35] S. J. Brodsky and S. Gardner, Phys. Rev. Lett. **116**, 019101 (2016).
  - [36] G. Bailas and V. P. Goncalves, Eur. Phys. J. C **76**, 105 (2016).
  - [37] T. Boettcher, P. Ilten and M. Williams, Phys. Rev. D **93**, 074008 (2016).
  - [38] F. Lyonnet, A. Kusina, T. Jezo, K. Kovarik, F. Olness, I. Schienbein and J. Y. Yu, JHEP **1507**, 141 (2015).
  - [39] S. Brodsky, F. Fleuret, C. Hadjidakis, and J. Lansberg, Phys. Rept. **522**, 239 (2013); J. Lansberg, S. Brodsky, F. Fleuret, and C. Hadjidakis, Few Body Syst. **53**, 11 (2012); J. Lansberg, R. Arnaldi, S. Brodsky, V. Chambert, J. Didelez, et al., EPJ Web Conf. **66**, 11023 (2014); A. Rakotozafindrabe, M. Anselmino, R. Arnaldi, E. Scapparini, S. Brodsky, et al., PoS **DIS2013**, 250 (2013).
  - [40] F. Halzen, Y. S. Jeong and C. S. Kim, Phys. Rev. D **88**, 073013 (2013); F. Halzen and L. Wille, arXiv:1601.03044; F. Halzen and L. Wille, Phys. Rev. D **94**, 014014 (2016).
  - [41] R. Gauld, J. Rojo, L. Rottoli, S. Sarkar and J. Talbert, JHEP **1602**, 130 (2016).
  - [42] F. Gelis, E. Iancu, J. Jalilian-Marian and R. Venugopalan, Ann. Rev. Nucl. Part. Sci. **60**, 463 (2010); E. Iancu and

- R. Venugopalan, arXiv:hep-ph/0303204; H. Weigert, Prog. Part. Nucl. Phys. **55**, 461 (2005); J. Jalilian-Marian and Y. V. Kovchegov, Prog. Part. Nucl. Phys. **56**, 104 (2006); J. L. Albacete and C. Marquet, Prog. Part. Nucl. Phys. **76**, 1 (2014).
- [43] A. Dumitru, A. Hayashigaki and J. Jalilian-Marian, Nucl. Phys. A **765**, 464 (2006); Nucl. Phys. A **770**, 57 (2006).
- [44] D. Boer, A. Utermann, E. Wessels, Phys. Rev. D **77**, 054014 (2008).
- [45] F. O. Durães, A. V. Giannini, V. P. Goncalves and F. S. Navarra, Phys. Rev. C **94**, 024917 (2016).
- [46] R. Gauld and J. Rojo, Phys. Rev. Lett. **118**, 072001 (2017).
- [47] N. N. Nikolaev, G. Piller and B. G. Zakharov, J. Exp. Theor. Phys. **81**, 851 (1995) [Zh. Eksp. Teor. Fiz. **108**, 1554 (1995)]; Z. Phys. A **354**, 99 (1996).
- [48] B. Z. Kopeliovich and A. V. Tarasov, Nucl. Phys. A **710**, 180 (2002).
- [49] V. P. Goncalves, B. Kopeliovich, J. Nemchik, R. Pasechnik and I. Potashnikova, Phys. Rev. D **96**, no. 1, 014010 (2017)
- [50] R. Maciula and A. Szczurek, Phys. Rev. D **87**, 094022 (2013).
- [51] P. Kotko, K. Kutak, C. Marquet, E. Petreska, S. Sapeta and A. van Hameren, JHEP **1509**, 106 (2015).
- [52] J. Raufeisen and J. C. Peng, Phys. Rev. D **67**, 054008 (2003).
- [53] F. O. Duraes, A. V. Giannini, V. P. Goncalves and F. S. Navarra, Phys. Rev. C **89**, 035205 (2014).
- [54] I. Balitsky, Nucl. Phys. B **463**, 99 (1996); Y. V. Kovchegov, Phys. Rev. D **60**, 034008 (1999); Phys. Rev. D **61**, 074018 (2000).
- [55] T. Lappi and H. Mantysaari, Phys. Rev. D **91**, 074016 (2015).
- [56] D. Kharzeev, Y.V. Kovchegov and K. Tuchin, Phys. Lett. **B599**, 23 (2004); J. Bartels, K. Golec-Biernat, H. Kowalski, Phys. Rev. D **66**, 014001 (2002); H. Kowalski and D. Teaney, Phys. Rev. D **68**, 114005 (2003); E. Iancu, K. Itakura, S. Munier, Phys. Lett. **B590**, 199 (2004); H. Kowalski, L. Motyka and G. Watt, Phys. Rev. D **74**, 074016(2006); V. P. Goncalves, M. S. Kugeratski, M. V. T. Machado and F. S. Navarra, Phys. Lett. B **643**, 273 (2006); C. Marquet, R. Peschanski and G. Soyez, Phys. Rev. D **76**, 034011 (2007); G. Soyez, Phys. Lett. B **655**, 32 (2007); G. Watt and H. Kowalski, Phys. Rev. D **78**, 014016 (2008).
- [57] R. Aaij *et al.* [LHCb Collaboration], Nucl. Phys. B **871**, 1 (2013).
- [58] R. Aaij *et al.* [LHCb Collaboration], JHEP **1603**, 159 (2016).
- [59] B. A. Kniehl and G. Kramer, Phys. Rev. D **74**, 037502 (2006).
- [60] B. A. Kniehl, G. Kramer, I. Schienbein and H. Spiesberger, Eur. Phys. J. C **72**, 2082 (2012)
- [61] I. Abt *et al.* [HERA-B Collaboration], Eur. Phys. J. C **52**, 531 (2007).
- [62] L. Adamczyk *et al.* [STAR Collaboration], Phys. Rev. D **86**, 072013 (2012).
- [63] B. Abelev *et al.* [ALICE Collaboration], JHEP **1211**, 065 (2012).
- [64] R. Aaij *et al.* [LHCb Collaboration], Eur. Phys. J. C **71**, 1645 (2011).